

# Breakthrough of Single-Quantum Signal in Double-Quantum Filtering and its Elimination

정 판 전<sup>1)</sup>, J. Katz<sup>2)</sup>, S.K. Hilal<sup>2)</sup>, 조 장 희<sup>3)</sup>

1) 전자부품 종합기술연구소, CATV 개발실; 2) 미국 Columbia 대학, 방사선과; 3) 한국과학기술원 서울분원, 정보 및 통신공학과

K.J. Jung<sup>1)</sup>, J. Katz<sup>2)</sup>, S.K. Hilal<sup>2)</sup>, and Z.H. Cho<sup>3)</sup>

1) CATV Project Management Office, Korea Electronics Technology Institute, Seoul; 2) Department of Radiology, Columbia University, New York, NY 10032, USA; 3) Dept. of Information and Communication Engineering, KAIST, Seoul Campus

### Abstracts

Breakthrough of single-quantum coherence is shown to occur even after application of a double-quantum filter with Bax's four-step phase-cycling scheme. The reason for this breakthrough is investigated and a method for its elimination is theoretically developed and experimentally demonstrated.

### Introduction

In a double-quantum (DQ) filtering experiment with the Bax's phase-cycled DQ filtering sequence (1)

$$90^\circ_\phi - \tau - 180^\circ_\phi - \tau - 90^\circ_\phi - \delta - 90^\circ - 2\delta - \text{Acq}_\psi$$

there is breakthrough of single-quantum coherence within both the acquired signal itself and the averaged signal by the DQ filtering scheme (2). We note that the single-quantum signal persisting after application of a DQ filter is an inter-sequence stimulated echo (STE), which is generated by the multiple  $90^\circ$  rf pulses in the preceding pulse sequences (3).

### Methods

**a) Inter-sequence STE:** The inter-sequence STE of interest is generated and refocused by the second and third (mixing)  $90^\circ$  rf pulses in the DQ filtering pulse sequence as shown in Fig. 1(a). The generation of the inter-sequence STE can be well explained by applying the phase diagram and the partition methods developed by J. Hennig and R. Kaiser et al. as illustrated in Figs. 1(b) and 1(c), respectively (4, 5). The spin is excited by the  $90^\circ$  rf pulse of the previous sequence and dephases during the DQ evolution time  $\delta$ . After the mixing rf pulse of the previous sequence is applied, the spin's phase on the transverse plane is stored and the spin experiences only the  $T_1$  relaxation until the next pulse sequence as illustrated by the horizontal line in Fig. 1(b). When the second  $90^\circ$  rf pulse of the current sequence is excited, the stored phase begins to dephase again during the DQ evolution time  $\delta$  in the same sense as in the previous sequence. When the mixing rf pulse of the current sequence is excited, the spin's phase is inverted and begins to rephase forming an echo at time  $2\delta$  after the mixing rf pulse.

This procedure can also be explained by the partition method as in Fig. 1(c), where the echo is formed when the sum of the subscripts equals to zero. The magnetization  $M_{101-2}$  after the mixing rf pulse of the current sequence corresponds to the inter-sequence STE which is generated from the previous sequence.

**b) Properties of inter-sequence STE:** The phases of inter-sequence STE's in the pulse sequence of Fig. 1(a) are calculated for Bax's four-step phase-cycling scheme by using the rotation operators as listed in Table 1. Note that the phases of inter-sequence STE's alternate between  $0^\circ$  and  $180^\circ$  as the rf phase  $\phi$  is rotated by  $90^\circ$  each step, resulting in the constructive addition by DQ filtering.

Another property is that for the inter-sequence STE the field inhomogeneity during the DQ evolution time  $\delta$  of the previous pulse sequence accumulates to that of the current pulse sequence with the same polarity as illustrated in Fig.

1(b). Therefore, the inter-sequence STE is refocused at time  $2\delta$  after the mixing rf pulse, i.e., at the same time as the DQ coherence signal.

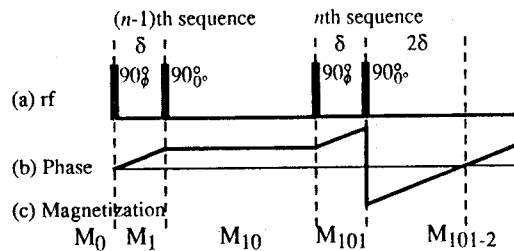


Fig. 1. Generation of inter-sequence STE in DQ filtering. (a) Simplified rf pulse sequence of a DQ filter. Only the last two  $90^\circ$  rf pulses, separated by the DQ evolution time  $\delta$ , are considered. (b) Phase diagram of the inter-sequence STE signal. (c) Evolution of the magnetization (represented by the subscripts) for the inter-sequence STE.

**c) New phase-cycling scheme:** Since the phase of the inter-sequence STE is determined by the rf phases of the previous and current pulse sequences, it can be controlled by changing the phase-cycling scheme. In the conventional Bax's phase-cycling scheme, the rf phase is rotated constantly in the positive direction, i.e.,  $[0^\circ, 90^\circ, 180^\circ, -90^\circ]$ . By inverting the rotating direction, i.e.,  $[0^\circ, -90^\circ, 180^\circ, 90^\circ]$ , the inter-sequence STE should experience a different phase. The phase of the inter-sequence STE calculated for the rf phase with the negative rotation is shown in Table 2. As expected, the phases for the negative rotation are shifted by  $180^\circ$  from those for the positive rotation.

Therefore, the inter-sequence STE can be eliminated by use of an eight-step phase-cycling scheme: four steps in the positive rotation followed by another four steps in the negative rotation, i.e.,  $[0^\circ, 90^\circ, 180^\circ, -90^\circ, 0^\circ, -90^\circ, 180^\circ, 90^\circ]$ .

The preceding arguments are valid only for two consecutive pulse sequences. In general, the inter-sequence STE may be generated from all the preceding pulse sequences, which may be eliminated by a more complicated phase-cycling scheme. However, since  $T_1$  relaxation is almost completed after  $2T_R$  ( $T_R$ : pulse repetition time), any additional STE contributions due to further earlier pulse sequences would be expected to be negligible.

**d) Computer simulation:** The aforementioned two kinds of phase-cycling schemes were tested by computer simulation. The simulation is done for the simplified rf pulse sequence of Fig. 1(a) by using the rotation matrix. A set of spins are assumed to have a uniform distribution of inhomogeneity neglecting  $T_1$  and  $T_2$  relaxation. The inter-sequence effects from the three consecutive pulse sequences are shown in Figs. 2(a) to 2(c), respectively, for various phase-cycling schemes: (a) no phase-cycling, (b) the conventional

Bax's four-step phase-cycling, and (c) the here proposed eight-step phase-cycling scheme. In the calculations, the DQ evolution time  $\delta$  between the two rf pulses has been taken to be 10 and  $T_R$  to be 100 in arbitrary units.

In Fig. 2(a) the primary spin echo is formed at  $t = 20$  and the inter-sequence stimulated echoes are formed at  $t = 130$  and 230. As shown in Fig. 2(b), when the Bax's four-step phase-cycling scheme is employed, the primary spin echo is eliminated but the inter-sequence STE's at  $t = 130$  and 230 remain just as in Fig. 2(a). With the phase-cycling scheme here proposed the inter-sequence STE at  $t = 130$  is eliminated as shown in Fig. 2(c). As expected, however, the inter-sequence STE at  $t = 230$  still remains.

These computer simulations clarify why the inter-sequence STE's are not filtered out by the conventional phase-cycling scheme while the inter-sequence STE caused by the previous pulse sequence can be filtered out by the phase-cycling scheme here proposed.

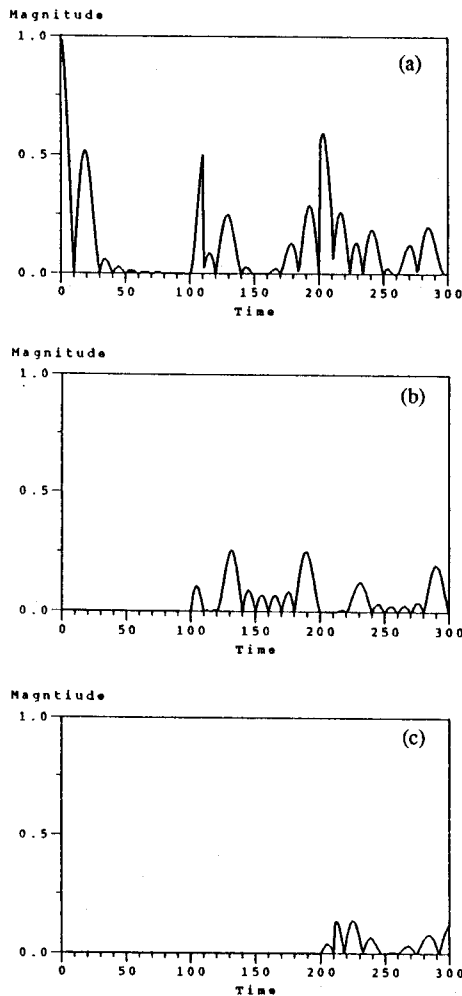


Fig. 2. Computer simulations for the simplified rf pulse sequence in Fig. 1(a). (a)  $\phi$  is always  $0^\circ$ . (b)  $\phi$  is cycled following the Bax's four-step cycling scheme, i.e.,  $[0^\circ, 90^\circ, 180^\circ, -90^\circ]$ . (c)  $\phi$  is cycled following the eight-step cycling scheme here proposed, i.e.,  $[0^\circ, 90^\circ, 180^\circ, -90^\circ, 0^\circ, -90^\circ, 180^\circ, 90^\circ]$ .

Table 1. Phases of the inter-sequence STE signals for the Bax's four-step phase-cycling scheme with a positive rotation of the rf phase  $\phi$ . Phases are measured relative to the  $x$  axis. The inter-sequence STE signals before and after multiplication by the receiver phase  $\psi$  of the DQ filter are denoted by  $S_T$  and  $S_T'$ , respectively.

$\phi$	$-90^\circ$	$0^\circ$	$90^\circ$	$180^\circ$	$-90^\circ$
$\psi$	$0^\circ$	$180^\circ$	$0^\circ$	$180^\circ$	$0^\circ$
phase of $S_T$	$180^\circ$	$0^\circ$	$180^\circ$	$0^\circ$	$0^\circ$
phase of $S_T'$	$180^\circ$	$180^\circ$	$180^\circ$	$180^\circ$	$180^\circ$

Table 2. Same as Table 1, but with a negative rotation of the rf phase  $\phi$ .

$\phi$	$90^\circ$	$0^\circ$	$-90^\circ$	$180^\circ$	$90^\circ$
$\psi$	$0^\circ$	$180^\circ$	$0^\circ$	$180^\circ$	$0^\circ$
phase of $S_T$	$0^\circ$	$180^\circ$	$0^\circ$	$180^\circ$	$180^\circ$
phase of $S_T'$	$0^\circ$	$0^\circ$	$0^\circ$	$0^\circ$	$0^\circ$

e) **Spoiling rf pulse:** In our experience, the inter-sequence STE signal is greater than the DQ coherence signal and, thereby, the dynamic range of the receiver is restricted by the inter-sequence STE signal and not by the DQ coherence signal. Even though the dynamic range of the receiver's ADC (analog-to-digital conversion) is sufficient, the dominant inter-sequence STE signal will make DQ filtering more subjective to instability and unbalance of the receiver.

Therefore, if possible, it is beneficial to reduce the inter-sequence STE signal before data acquisition. For this purpose, a spoiling rf pulse followed by dephasing gradient pulses can be applied to the DQ filtering pulse sequence as shown in the experimental pulse sequence of Fig. 3. The effects of the spoiling rf pulse are to disperse the phase transition and the magnetization components leading to the inter-sequence STE in Figs. 1(b) and 1(c), respectively, so that the contribution to the inter-sequence STE at time  $2\delta$  could be reduced.

## Experiments and Discussion

By using a home-built NMR system with a 3 tesla magnet, experiments were done to investigate the properties of the inter-sequence STE and to compare the results of the conventional and here proposed phase-cycling schemes. We obtained 1-D profiles of a phantom consisting of three 5 cc syringes containing water doped with  $\text{CuSO}_4$ , 40% lactate (about 3.7 M), and corn oil, respectively. The measured  $T_1$  relaxation constants were 882 ms, 760 ms, and 234 ms for water, lactate, and corn oil, respectively.

We used the slice-selective DQ filtering pulse sequence shown in Fig. 3 with a slice-selective refocusing  $180^\circ$  rf pulse. The first  $90^\circ$  rf pulse may also be slice-selective. However, we used only a slice-selective  $180^\circ$  rf pulse because the slice-selective gradient pulse for the  $180^\circ$  rf pulse could be better balanced than the one for the first  $90^\circ$  rf pulse.

The creation time  $2\tau$  was set to 72 ms with the assumed  $J$  of 7 Hz for lactate (6). The DQ coherence evolution time  $\delta$  was minimized (8 ms) so that dephasing due to the  $J$ -coupling during the time  $2\delta$  after the mixing rf pulse could be minimized. The limiting factor in shortening  $\delta$  was the readout gradient pulse applied during the DQ evolution time  $\delta$ . The

area of the readout gradient applied for time  $2\delta$  after the mixing rf pulse should be two times the area applied during the DQ evolution time  $\delta$ . Furthermore, the readout gradient after the mixing rf pulse should be long enough to suppress the FID and echo signals arising after the mixing rf pulse. The additional  $90^\circ$  rf pulse after the data acquisition is a spoiling rf pulse, which is followed by dephasing gradient pulses in both the slice-selective and readout directions.

First, by varying the pulse repetition time  $T_R$  from 0.5 sec to 4.0 sec, the effects of  $T_R$  on the inter-sequence STE were studied with the conventional phase-cycling scheme as shown in Fig. 4. The spoiling rf pulse was not applied. In Fig. 4 it is apparent that the doped water signal is quite large at  $T_R = 0.5$  sec, which shows that the single-quantum signal is present even after DQ filtering. As  $T_R$  is increased, the single-quantum signal decreases. In particular, the water signal decreases fast as  $T_R$  is increased and is almost nullified at  $T_R = 4.0$  sec. The decrease of the single-quantum signal as  $T_R$  is increased is due to increased  $T_1$  relaxation during  $T_R$ . Conversely, the inter-sequence STE increases as  $T_R$  is decreased because of less  $T_1$  relaxation during  $T_R$ . On the other hand, the signal of corn oil does not vary much for the different  $T_R$ 's, which is reasonable considering the short  $T_1$  of oil: corn oil relaxes fast during  $T_R$  and yields a negligible contribution to the inter-sequence STE signal.

Second, we compared the here proposed phase-cycling scheme with the conventional one for  $T_R = 0.5$  sec, as shown in Fig. 5. The spoiling rf pulse was not employed. The single-quantum signal was much more suppressed by the phase-cycling scheme here proposed than by the conventional one.

Third, the above step was repeated in the presence of a spoiling rf pulse. Since, as mentioned in the methods section, the signal on the acquisition window was then much reduced, the signal attenuator was decreased by 12 dB. Furthermore, even with the conventional phase-cycling scheme, water signals were less than the corresponding signals obtained without a spoiling rf pulse, as shown in Fig. 6(a). Again, a water signal was present with the conventional phase-cycling scheme while it was eliminated with the phase-cycling scheme here proposed as shown in Fig. 6(b).

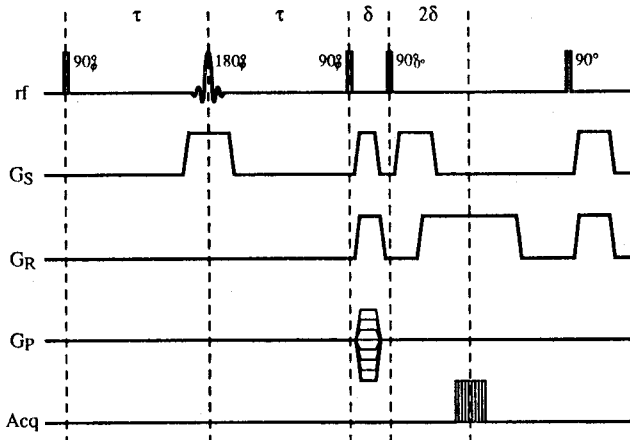


Fig. 3. DQ filtering pulse sequence.  $G_S$ ,  $G_R$ , and  $G_P$  denote the slice-selective, readout, and phase-encoding gradients, respectively. The last  $90^\circ$  is the spoiling rf pulse. The amplitude of the phase-encoding gradient  $G_P$  is half of that for the single-quantum case.

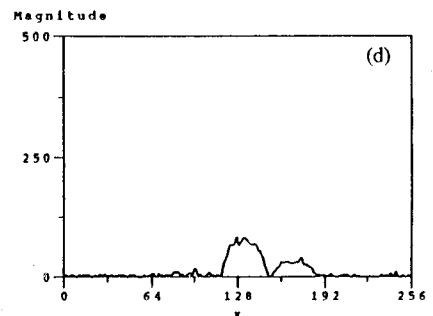
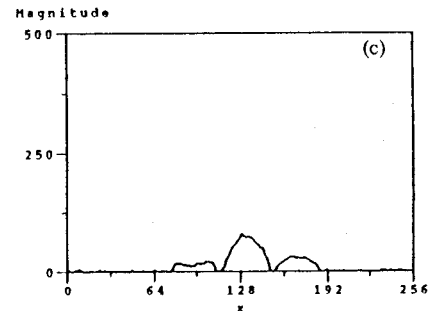
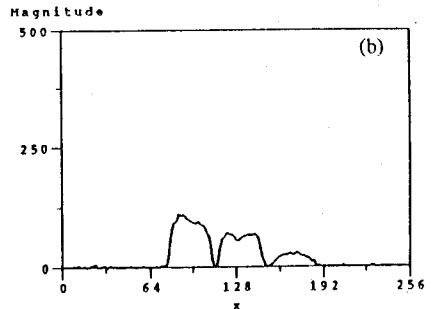
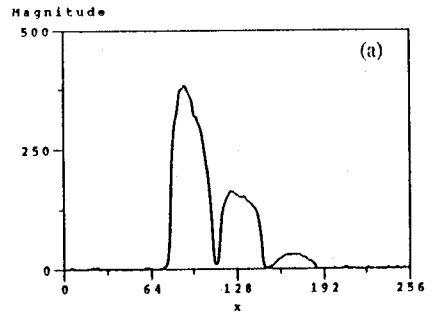


Fig. 4. 1-D profiles of the phantom for various  $T_R$ 's. From left to right, the phantom contains water, lactate, and corn oil.  $T_R$ 's used in (a) to (d) were 0.5, 1.0, 2.0 and 4.0 sec, respectively.

## Conclusions

Breakthrough of single-quantum coherence is here shown to occur after application of a DQ filter due to the inter-sequence stimulated echo generated by the rf pulses in the preceding pulse sequences. This single-quantum signal can be eliminated by the phase-cycling scheme here proposed, which is a generalization of the Bax's four-step phase-cycling scheme. Furthermore, application of a spoiling rf pulse followed by dephasing gradients is shown to reduce the inter-sequence stimulated echo and thereby increase the dynamic range of the receiver electronics.

Even though the phase-cycling scheme here proposed is designed to suppress the inter-sequence stimulated echo generated from the previous pulse sequence, a similar analysis method can be used to develop alternative phase-cycling schemes to eliminate, in general, the inter-sequence stimulated echoes in a given pulse sequence arising from pulse sequences earlier than the previous one. Practically, however, this will not be necessary since  $T_1$  relaxation is almost completed after  $2T_R$ , so that additional stimulated echo contributions due to those additional pulse sequences should be expected to be negligible. The principle here discussed may also be applied to the elimination of single-quantum coherence which persists after application of multiple-quantum filters for higher orders of coherences.

## References

1. A. Bax, R. Freeman, and S.P. Kempell, *J. Am. Chem. Soc.* 102, No. 14, 4849-4851 (1980).
2. L. Braunschweiler, G. Bodenhausen, and R.R. Ernst, *Molecular Phys.* 48, No. 3, 535-560 (1983).
3. E.L. Han, *Physical Review* 80, No. 4, 580-594 (1950).
4. R. Kaiser, E. Bartholdi, and R.R. Ernst, *J. Chem. Phys.* 60, No. 8, 2966-2979 (1974).
5. J. Hennig, *J. Magn. Reson.* 78, 397-407 (1988).
6. N.M. Szeverenyi and E.M. Haacke, *J. Computer Assisted Tomogr.* 10(3), 484-489 (1986).

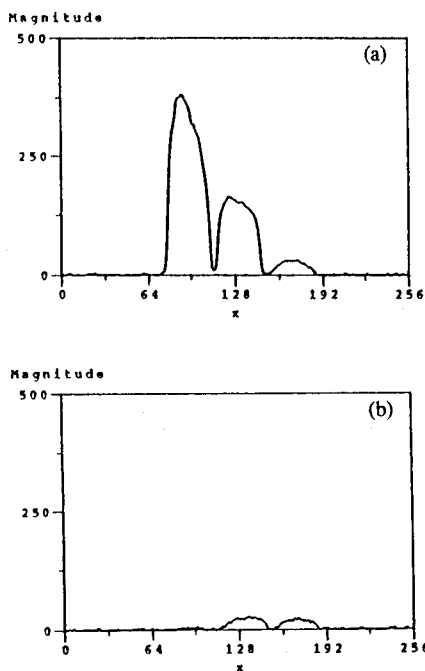


Fig. 5. Comparison of the conventional and here proposed phase-cycling schemes by obtaining the 1-D profiles of the phantom without a spoiling rf pulse. (a) was obtained with the conventional phase-cycling scheme, while (b) with the phase-cycling scheme here proposed.

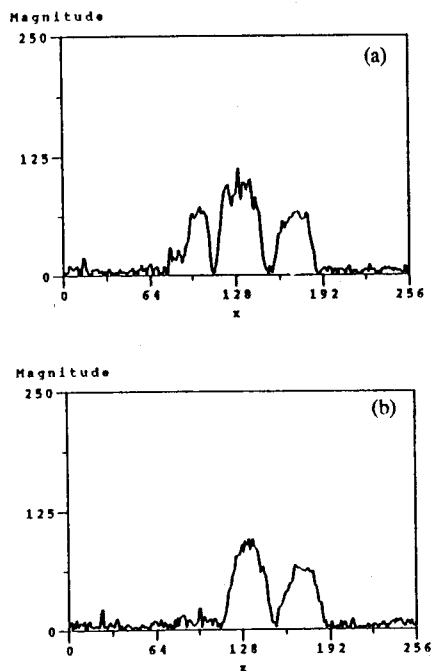


Fig. 6. Same as in Fig. 5, but with the spoiling rf pulse applied.